Author Manuscript

Author Manuscript

Author Manuscript

Author Manuscript

HHS Public Access

Author manuscript

Solid State Nucl Magn Reson. Author manuscript; available in PMC 2019 August 01.

Published in final edited form as:

Solid State Nucl Magn Reson. 2018 August ; 92: 1–6. doi:10.1016/j.ssnmr.2018.03.002.

Backbone Amide ^{15}N Chemical Shift Tensors Report on Hydrogen Bonding Interactions in Proteins: A Magic Angle Spinning NMR Study

Sivakumar Paramsivam[1,2,*], **Angela M. Gronenborn**[3,4], and **Tatyana Polenova**[2,4,*]

[1]Present address: Department of Physics and Nanotechnology, SRM Institute of Science and Technology, Kattankulathur, Chennai 603 203, India;

[2]Department of Chemistry and Biochemistry, University of Delaware, Newark, DE 19716, United States;

[3]Department of Structural Biology, University of Pittsburgh School of Medicine, Pittsburgh, PA 15260, United States;

[4]Pittsburgh Center for HIV Protein Interactions, University of Pittsburgh, Pittsburgh, PA 15260, United States

Abstract

Chemical shift tensors (CSTs) are an exquisite probe of local geometric and electronic structure. ^{15}N CST are very sensitive to hydrogen bonding, yet they have been reported for very few proteins to date. Here we present experimental results and statistical analysis of backbone amide ^{15}N CSTs for 100 residues of four proteins, two *E. coli* thioredoxin reassemblies (1–73-(U-^{13}C,^{15}N)/74–108-(U-^{15}N) and 1–73-(U-^{15}N)/74–108-(U-^{13}C,^{15}N)), dynein light chain 8 LC8, and CAP-Gly domain of the mammalian dynactin. The ^{15}N CSTs were measured by a symmetry-based CSA recoupling method, ROCSA. Our results show that the principal component δ_{11} is very sensitive to the presence of hydrogen bonding interactions due to its unique orientation in the molecular frame. The downfield chemical shift change of backbone amide nitrogen nuclei with increasing hydrogen bond strength is manifested in the negative correlation of the principal components with hydrogen bond distance for both α-helical and β-sheet secondary structure elements. Our findings highlight the potential for the use of ^{15}N CSTs in protein structure refinement.

Keywords

magic-angle spinning NMR; chemical shift tensor; hydrogen bonding; proteins

1. INTRODUCTION

Hydrogen bond (HB) is one of the important noncovalent interactions stabilizing folded proteins [1]. NMR spectroscopy has long been used in the identification of hydrogen bonds

[*]**Corresponding authors:** Sivakumar Paramasivam, Department of Physics and Nanotechnology, SRM Institute of Science and Technology, Kattankulathur, Chennai 603 203, India, sivakumar.param@gmail.com, Tel. (0)94860 91214; Tatyana Polenova, Department of Chemistry and Biochemistry, University of Delaware, Newark, DE 19716, tpolenov@udel.edu, Tel. (302) 831-1968.

Author Manuscript Author Manuscript Author Manuscript Author Manuscript

in peptides and proteins through a number of NMR parameters. In particular, solution NMR signatures include chemical shift changes of the nuclei participating in HB interactions, reduced amide proton exchange rates, and indirect scalar or *J*-couplings mediated across hydrogen bonds to identify residues involved in hydrogen bonds. Among these, chemical shift perturbations are the easiest to measure directly using multidimensional homonuclear and heteronuclear correlation spectroscopy, as chemical shift parameters are highly sensitive to the local changes in the electronic environment due to HB interactions.

While solution NMR methods yield only the isotropic chemical shifts, in solid-state NMR (SSNMR) chemical shift tensors (CSTs) can be recorded. Chemical shift anisotropy (CSA) can be measured for multiple sites in a site-specific manner using magic angle spinning (MAS) NMR spectroscopy, where a chemical shift recoupling sequence is introduced into multidimensional experiments [2]. Yet, the literature on CSTs in proteins is sparse [3; 4] and the general rules governing the dependence of CST principal components on HB interactions remain to be established. For instance, the downfield change in the isotropic chemical shift due to the deshielding of amide protons involved in hydrogen bonds has been very well documented in the literature [5; 6; 7]. Recently our group reported site-specific amide proton CSA measurements for CAP-Gly domain of the mammalian dynactin, using the RN-symmetry based sequences [4]. The results revealed that indeed there is a high degree of correlation between the downfield shift of the principal components of the amide proton CST and the hydrogen bond length. Direct ^{1}H–^{15}N dipolar recoupling measurements have also been sometimes used in the literature to identify hydrogen bonds in terms of the elongation of N-H bond vector [8].

There have also been reports in the literature on the sensitivity of heteronuclear CS parameters to HB interactions in peptides and amino acids. In particular, the CSTs of both carbonyl carbon and amide nitrogen nuclei are as sensitive to HBs as amide protons. In an early SSNMR study of L-alanine containing short peptides, Asakawa et al. showed that as the hydrogen bond strength increases with decreasing distance between the nitrogen and oxygen atom ($R_{N\cdots O}$), the principal component δ_{22} of the carbonyl carbon shows a large downfield shift accompanied by a similar trend in the isotropic chemical shift [9]. In a more detailed SSNMR study of CSA of carboxyl groups of amino acids, Gu et al. demonstrated the unique sensitivity of δ_{11} and δ_{22} to the protonation state and HB interaction of the CO group, respectively [10]. In a DFT study of model dipeptides, Walling et al. showed that, in addition to carbonyl atoms, backbone amide ^{15}N CST parameters are also sensitive to hydrogen bonds [11]. In particular, they showed that both δ_{11} and δ_{33} exhibit downfield shift in both α-helical and β-sheet conformation, while δ_{22} displays upfield shift in β-sheet conformation. This trend is consistent with ^{15}N CST calculations performed on other model systems such as benzamide [12]. In contrast, a downfield shift of δ_{22} with increasing $R_{N\cdots O}$ and negligible sensitivity to HBs in both δ_{11} and δ_{33} was observed for the ^{15}N nuclei of imidazole groups in histidines by Wei et al. [13], which is in agreement with results from ^{15}N solution NMR studies of imidazoles [14]. Altough the magnitudes of the principal components of ^{15}N CST are very sensitive to HB interactions, the orientation of the ^{15}N CSTs in the molecular frame has been reported to be generally unperturbed on hydrogen bonding [15].

Author Manuscript Author Manuscript Author Manuscript Author Manuscript

Despite the vast amount of theoretical and experimental-SSNMR studies of hydrogen bond effect on both ^{15}N and ^{13}C CST parameters on amino acids and model peptides, the corresponding experimental investigations in large systems, such as proteins are lacking. In this work, we present experimental SSNMR results and a statistical analysis of backbone amide ^{15}N CST parameters for a total of 100 residues belonging to four proteins, two *E. coli* thioredoxin reassemblies ((1–73-(U-^{13}C,^{15}N)/74–108-(U-^{15}N) and 1–73-(U-^{15}N)/74–108-(U-^{13}C,^{15}N)), dynein light chain 8 LC8, and CAP-Gly domain of the mammalian dynactin. The ^{15}N CST parameters measured by the ROCSA symmetry based recoupling are interpreted in terms of their sensitivity to HB interactions of the residues. Our results reveal unequivocal correlation between the principal components of the backbone ^{15}N chemical shift tensors and hydrogen bonding interactions, underscoring the potential for use of ^{15}N CSTs in protein structure refinement.

2. EXPERIMENTS AND METHODS

2.1. Protein samples preparation.

Preparation of solid-state NMR samples of *E. coli* thioredoxin reassemblies [1–73-(U-^{13}C, ^{15}N)/74–108-(U-^{15}N) and 1–73-(U-^{15}N)/74–108-(U-^{13}C,^{15}N)], U-^{13}C/^{15}N DLC8, and U-^{13}C/^{15}N CAP-Gly domain of the mammalian dynactin by controlled precipitation was reported previously [16; 17; 18]. Approximately 10 mg of each sample was packed into a 3.2 mm Varian MAS rotor and sealed with an upper spacer and a top spinner.

2.2. SSNMR spectroscopy.

All SSNMR spectra presented in this work were acquired at 14.1 T on a narrow bore Varian InfinityPlus spectrometer operating at Larmor frequencies of 599.8 MHz for ^{1}H, 150.8 MHz for ^{13}C, and 60.8 MHz for ^{15}N. The instrument was outfitted with a 3.2 mm T3 MAS probe. The MAS frequency was 10 kHz for all experiments, and was controlled to within ±1 Hz by a Varian MAS controller. The sample temperatures were kept in the range 0 ^{o}C to –15 ^{o}C. The temperature reported includes a MAS frequency-dependent correction determined experimentally by using $PbNO_3$ as the temperature sensor [19]. ^{15}N chemical shifts were referenced with respect to NH_4Cl used as an external referencing standard following the standard protocol [20]. The ^{15}N CSA recoupling was achieved by the symmetry-based ROCSA method [21]. The pulse sequence for the 3D NCA-ROCSA experiment is shown in Figure 3. The excitation frequencies were set at 122.4 ppm for ^{15}N and at 55.5 ppm for ^{13}C. Eighteen ROCSA points were acquired with the dwell time equal to one rotor period, and 64 ^{15}N t_2 points with acquired with the dwell time of 120 μs. 128 scans were added to record each point in the indirect dimensions of the 3D spectra. ^{1}H 90 pulse width was 2.78 μs. The contact time for the ^{1}H-^{15}N CP was 1.6 ms. The ^{1}H radio frequency field strength was 51 kHz, the ^{15}N field was linearly ramped 70–100% with the center of the ramp being 41 kHz. The ROCSA sequence was used with a window τ_a of 3.29 μs, and 42.8 kHz rf irradiation was employed. The Z-filter pulses were placed after the ROCSA block; the rf field strength was 50 kHz. The Z-filter delay was set equal to one rotor period. XY-16 decoupling [22] on the ^{13}C channel was performed with the rf field strength of 50 kHz. 100 kHz CW decoupling was performed on the ^{1}H channel during ROCSA. SPECIFIC-CP [23] for ^{15}N-^{13}CA transfer was utilized. The ^{13}C field was tangentially ramped 90–100% with the center of the ramp

Author Manuscript Author Manuscript Author Manuscript Author Manuscript

being 35 kHz; the rf field strength for ^{15}N was 25 kHz; the contact time was 6.2 ms. 100 kHz CW decoupling was applied during SPECIFIC-CP. The Z-filter pulses were incorporated on the ^{13}C channel immediately after SPECIFIC-CP; the rf field strength was 67.9 kHz. 90 kHz TPPM decoupling [24] was applied during the t_3 evolution; the TPPM pulse width was 5.4 μs.

2.3. ^{15}N ROCSA lineshape simulations.

Numerical simulations of the ROCSA lineshapes were performed on a single ^{15}N spin using SIMPSON [25] with repulsion 320 powder angle set [26] and 36 γ-angles. An ideal ^{1}H-^{15}N cross polarization and proton decoupling during ROCSA evolution was assumed. The ROCSA lineshapes were fitted using MINUIT with the SIMPLEX method with three adjustable parameters: i) reduced anisotropy (δ_σ); ii) asymmetry parameter (η_σ); and iii) exponential line-broadening parameter to model transverse relaxation during ^{15}N ROCSA evolution. The uncertainties in the fitting parameters were determined using the Monte Carlo method as described in the literature [27]. The principal components of the ^{15}N CS tensors in the standard convention ($\delta_{11} \geq \delta_{22} \geq \delta_{33}$) were determined using the relations, $\delta_{11} = \delta_{iso} + \delta_\sigma$, $\delta_{22} = \delta_{iso} - \delta_\sigma(1 - \eta_\sigma)/2$, and $\delta_{33} = \delta_{iso} - \delta_\sigma(1 + \eta_\sigma)/2$.

2.4. Hydrogen bond analysis.

The hydrogen bond information of residues in the *E. coli* thioredoxin reassembly was inferred from its 1.8 Å crystal structure (PDB ID 2TRX) [28]. For LC8, a 2.8 Å resolution crystal structure (PDB ID 2PG1) was used [29]. MAS NMR structure was used for CAP-Gly domain of the mammalian dynactin (PDB ID 2M02) [30]. In all cases, an upper cutoff distance of 3.5 Å was set for $R_{N\cdots O}$. Residues exhibiting significant dynamic averaging of ^{15}N CSA due to internal motions in the solid-state samples, such as G21, R73, and I75 of *E. coli* thioredoxin [31], were excluded from this analysis.

3. RESULTS AND DISCUSSION

3.1. Sensitivity of backbone amide ^{15}N CST to presence of hydrogen bonds.

As shown in Figure 1B for *E. coli* thioredoxin reassembly (U-^{15}N 1–73/^{13}C,^{15}N 74–108), the resolution of the NC chemical shift correlation plane of the 3D ROCSA-NCA spectrum is high permitting the extract the ROCSA lineshapes corresponding to the resolved peaks. In total, we have recorded ROCSA lineshapes for 100 residues in *E. coli* thioredoxin reassembly (U-^{13}C/^{15}N 1–73/^{15}N 74–108, U-^{15}N 1–73/^{13}C,^{15}N 74–108), dynein light chain 8 (LC8), and CAP-Gly domain of mammalian dynactin. The corresponding CST parameters are summarized in Table S1. Representative experimental and best-fit ROCSA lineshapes for *E. coli* thioredoxin reassembly (U-^{15}N 1–73/^{13}C,^{15}N 74–108) and LC8 are shown in Figure 2.

Downfield shift of the isotropic component of the CS tensor of amide protons and amide nitrogens is known to be a characteristic marker of HB interactions [5; 6; 7]. This trend is confirmed in our results by the comparison of the statistical average value of the isotropic chemical shifts of the hydrogen-bonded ^{15}N nuclei versus those that do not participate in hydrogen bonds. As shown in Table 1, the average isotropic chemical shift δ_{iso}, of the

Author Manuscript Author Manuscript Author Manuscript Author Manuscript

hydrogen bonded ^{15}N nuclei is around 120.6 ppm while that of the non-hydrogen-bonded ^{15}N is 118.9 ppm. The difference of 1.7 ppm is significant enough for the direct detection of the nuclei participating in H-bonds from the 1D ^{15}N CPMAS spectra or 2D correlation spectra, such as NCA or NCO.

The hydrogen bond interaction increases the width of ^{15}N CSA lineshapes, which can easily be measured from the width of the ROCSA patterns. The reduced anisotropy, δ_σ, of the ^{15}N CST exhibits the same trend as the isotropic chemical shifts. Specifically, the average δ_σ value of hydrogen bonded residues is 95.8 ppm while δ_σ of residues not forming hydrogen bonds is 93.6 ppm. Although the difference of 2.2 ppm is relatively small, it is statistically significant and exceeds the typical experimental errors associated with modern CSA recoupling sequences designed for MAS frequencies exceeding 10 kHz, such as ROCSA and RNCSA [3]. Unlike δ_{iso} and δ_σ, the asymmetry parameter of the ^{15}N CSA tensor (η_σ) is not sensitive to hydrogen bond interaction. The average η_σ values of both hydrogen-bonded and non-hydrogen-bonded ^{15}N nuclei are essentially the same 0.2.

More insight into the sensitivity of the individual components of the CSA tensor to the hydrogen bonding interactions can be gained from the analysis of the principal components using the standard convention, (δ_{11}, δ_{22}, δ_{33}). It is evident from Table 1 that the most downfield shifted component δ_{11} is the most sensitive to the presence of hydrogen bonds. The average δ_{11} value for hydrogen-bonded ^{15}N nuclei is 216.3 ppm, while it is 212.5 ppm for non-hydrogen-bonded residues. The component with intermediate shielding, δ_{22}, and the most shielded component δ_{33} of the ^{15}N CSA tensor show relatively minor downfield shift due to the presence of HB interactions. The average value of δ_{22} for hydrogen-bonded residues is 83.8 ppm and 83.3 ppm for the non-hydrogen-bonded residues. The corresponding values for δ_{33} are 61.5 and 61.0 ppm.

The result that the δ_{11} component of the ^{15}N CSA tensor has the highest sensitivity to hydrogen bonding is in perfect agreement with theoretical studies of ^{15}N shielding tensors on hydrogen bonded amino acids and peptides [15; 32]. In these studies, it has been shown that the orientation of the ^{15}N CS tensor relative to the molecular frame is such that the δ_{11} component lies in the peptide plane with the angle between the N–H bond vector and the δ_{11} component being around ca. 10–20 degrees (Figure 3). The almost parallel orientation of δ_{11} component with respect to the N–H bond vector gives it the highest perturbation due to hydrogen bond interaction. The δ_{22} component which shows weak sensitivity to hydrogen bond interactions lies almost perpendicular to the peptide plane. The equally weakly sensitive δ_{33} component lies in the peptide plane with almost perpendicular orientation to the N–H bond vector.

It is important to mention that the backbone amide ^{15}N CS tensors are not only sensitive to hydrogen bonds, but are also dependent on secondary structure, nature of the amino acid, and internal dynamics of backbone. This fact is evident in the large standard deviations associated with each of the three principal components for both hydrogen-bonded and non-hydrogen-bonded residues as presented in Table 1. Nevertheless, despite the limited number of ^{15}N CSA lineshapes available so far and analyzed in this work, we do observe a clear downfield shift in δ_{11} due to hydrogen bond interactions.

Author Manuscript Author Manuscript Author Manuscript Author Manuscript

3.2. Correlation of backbone amide ^{15}N CST components with isotropic chemical shift.

In the case of amide proton CSA parameters, Tjandra et al. reported the correlation of the three principal components with the isotropic chemical shift as an essential metric for the sensitivity of amide proton CSA parameters to HB interactions [5]. Recently, in our work on MAS NMR measurements of backbone amide proton CSTs of CAP-Gly domain of the mammalian dynactin, the correlation of the three principal components with the isotropic chemical of the backbone amide protons was verified to be correct [4]. In order to examine whether the same trend is observed for the backbone amide ^{15}N CST parameters, in Figure 4 we have plotted the three ^{15}N principal components versus the isotropic chemical shift. Similar to the findings for the backbone amide proton CSAs, ^{15}N CS principal components also follow a linear relationship with the isotropic chemical shift, with a strong positive correlation indicated by positive values of Pearson correlation coefficients of 0.73, 0.84, and 0.79 for δ_{11}, δ_{22}, and δ_{33} respectively. These results suggest that that one can expect to see a similar positive correlation of the three amide ^{15}N CSAs with hydrogen bond strength or a negative correlation with hydrogen bond distance. This assertion is corroborated in the following section.

3.3. Correlation of backbone amide ^{15}N CST with hydrogen bond length.

Ab initio theoretical and experimental studies have shown that CS tensor values of nuclei involved in hydrogen bond correlate well with hydrogen bond length values [7; 12]. In particular, the downfield shift of nuclei of the donor group with increasing hydrogen bond strength or decreasing hydrogen bond length ($R_{N\ldots O}$ or $R_{H\ldots O}$) due to increased deshielding has been well investigated [6; 7]. In this section, we present the statistical correlation of backbone amide ^{15}N CS principal components with the distance between the amide ^{15}N atom in the donor group and the oxygen atom in the acceptor group. As mentioned in the previous section, in addition to HB interactions backbone amide ^{15}N CST values are dependent on several other parameters such as secondary structure, local conformation and internal dynamics. In order to decouple the sensitivity of amide ^{15}N CST on secondary structure, we have performed two separate correlation analyses, one for α-helical residues, and the other for β-strand residues. The results are shown in Figure 5. Out of the 100 residues we have analyzed from the four proteins, 65 are hydrogen bonded and 35 are non-hydrogen bonded. Among the hydrogen-bonded, 21 are α-helical residues and 32 are located in β -strands.

In Figure 5, the correlation of the principal components of backbone amide ^{15}N CST is plotted against $R_{N\ldots O}$ for both α-helical and β -strand residues. First, a negative correlation as determined by the Pearson correlation coefficient is evident in all the graphs. This statistical observation is consistent with the fact that the downfield chemical shift change of backbone amide ^{15}N CST values correlate with decreasing hydrogen bond lengths as reported in literature [13]. Among the two secondary structure types, for α-helices, the δ_{11} component exhibits the highest sensitivity to the hydrogen bonding distance with R_P of –0.19. The δ_{22} component is somewhat less sensitive with R_P of –0.14, and δ_{33} has the smallest or almost no correlation (R_P equal to –0.04). This trend is in very good agreement with the assertion that the least-shielded component δ_{11} acquires maximum sensitivity due to its collinear orientation with the N-H bond vector.

Author Manuscript Author Manuscript Author Manuscript Author Manuscript

Interestingly, for β-strands, the δ_{33} component, which lies in the peptide plane with almost perpendicular orientation to the N-H bond vector, has the maximum negative correlation with R_P of –0.25 while the δ_{11} component is somewhat less sensitive with R_P equal to –0.16. The δ_{22} component shows the weakest correlation with R_P equal to –0.05. The less negative correlation of δ_{22} component with $R_{N\ldots O}$ for β-sheets is consistent with earlier reports that δ_{22} component is shifted upfield or shows positive correlation with increasing hydrogen bond strength or decreasing $R_{N\ldots O}$ [11]. However, the decreased sensitivity of δ_{11} and the increased sensitivity of δ_{33} to hydrogen bond length in β -strands is somewhat surprising. It would be interesting to explore this further through quantum chemical calculations of the hydrogen-bonded backbone amide ^{15}N chemical shift tensors as a function of the secondary structure type.

As shown in Figure 5, the magnitudes of the Pearson correlation coefficients are in the range of 0.04–0.19, which indicate only a modest correlation of backbone amide ^{15}N CST with hydrogen bond length. Despite these modest values of R_P, a clear trend of δ_{ii} (ii = 11, 22, 33) linearly decreasing with $R_{N\ldots O}$ is evident for both α-helical and β-strand secondary structure types.

4. CONCLUSIONS

We have presented experimental SSNMR data and statistical analysis of site-specific backbone amide ^{15}N CS tensor components of 100 residues of four different proteins, *E. coli* thioredoxin, DLC8 and CAP-Gly domain of the mammalian dynactin. Our results reveal that the least-shielded component δ_{11} of the backbone amide ^{15}N is very sensitive to hydrogen bond interaction, displaying a significant downfield shift. The downfield chemical shift change of backbone amide nitrogen nuclei with increasing hydrogen bond strength is manifested in the negative correlation of the principal components with hydrogen bond distance for both secondary structure elements, α-helices and β -sheets. Our results are consistent with the theoretical studies of ^{15}N shielding tensors on model compounds and short peptides. In order to improve this analysis further, one needs to record a larger database of ^{15}N chemical shift tensors, which would encompass multiple proteins and different secondary structure types. These studies are currently ongoing in our laboratory.

Supplementary Material

Refer to Web version on PubMed Central for supplementary material.

ACKNOWLEDGMENTS

This work was supported by the National Institutes of Health (NIH Grant P50 GM082251, Technology Development Project on MAS NMR). We acknowledge the support of the National Institutes of Health (NIH Grants P30GM103519 and P30GM110758) for the support of core instrumentation infrastructure at the University of Delaware.

REFERENCES

[1]. Baker EN, and Hubbard RE, Hydrogen bonding in globular proteins. Prog. Biophys. Mol. Biol. 44 (1984) 97–179. [PubMed: 6385134]

Author Manuscript Author Manuscript Author Manuscript Author Manuscript

[2]. Saitô H, Ando I, and Ramamoorthy A, Chemical Shift Tensor – the Heart of NMR: Insights into Biological Aspects of Proteins. Prog. Nucl. Magn. Reson. Spectrosc. 57 (2010) 181–228. [PubMed: 20633363]

[3]. Hou G, Byeon IJ, Ahn J, Gronenborn AM, and Polenova T, Recoupling of chemical shift anisotropy by R-symmetry sequences in magic angle spinning NMR spectroscopy. J. Chem. Phys. 137 (2012) 134201. [PubMed: 23039592]

[4]. Hou G, Paramasivam S, Yan S, Polenova T, and Vega AJ, Multidimensional magic angle spinning NMR spectroscopy for site-resolved measurement of proton chemical shift anisotropy in biological solids. J. Am. Chem. Soc. 135 (2013) 1358–68. [PubMed: 23286322]

[5]. Tjandra N, and Bax A, Solution NMR Measurement of Amide Proton Chemical Shift Anisotropy in 15N-Enriched Proteins. Correlation with Hydrogen Bond Length. Journal of the American Chemical Society 119 (1997) 8076–8082.

[6]. Yao L, Grishaev A, Cornilescu G, and Bax A, The Impact of Hydrogen Bonding on Amide (1)H Chemical Shift Anisotropy Studied by Cross-Correlated Relaxation and Liquid Crystal NMR Spectroscopy. J. Am. Chem. Soc. 132 (2010) 10866–75. [PubMed: 20681720]

[7]. Sharma Y, Kwon OY, Brooks B, and Tjandra N, An ab initio study of amide proton shift tensor dependence on local protein structure. J. Am. Chem. Soc. 124 (2002) 327–35. [PubMed: 11782185]

[8]. Zhao X, Sudmeier JL, Bachovchin WW, and Levitt MH, Measurement of NH bond lengths by fast magic-angle spinning solid-state NMR spectroscopy: a new method for the quantification of hydrogen bonds. J. Am. Chem. Soc. 123 (2001) 11097–8. [PubMed: 11686729]

[9]. Asakawa N, Kuroki S, Kurosu H, Ando I, Shoji A, and Ozaki T, Hydrogen-bonding effect on carbon-13 NMR chemical shifts of L-alanine residue carbonyl carbons of peptides in the solid state. Journal of the American Chemical Society 114 (1992) 3261–3265.

[10]. Wei Y, de Dios AC, and McDermott AE, Solid-State 15N NMR Chemical Shift Anisotropy of Histidines: Experimental and Theoretical Studies of Hydrogen Bonding. Journal of the American Chemical Society 121 (1999) 10389–10394.

[11]. Walling AE, Pargas RE, and de Dios AC, Chemical Shift Tensors in Peptides: A Quantum Mechanical Study. J. Phys. Chem. A 101 (1997) 7299–7303.

[12]. Facelli JC, Pugmire RJ, and Grant DM, Effects of Hydrogen Bonding in the Calculation of 15N Chemical Shift Tensors: Benzamide. Journal of the American Chemical Society 118 (1996) 5488–5489.

[13]. Wei Y, De Dios AC, and McDermott AE, Solid-state 15N NMR chemical shift anisotropy of histidines: Experimental and theoretical studies of hydrogen bonding. Journal of the American Chemical Society 121 (1999) 10389–10394.

[14]. Schuster II, and Roberts JD, Nitrogen-15 nuclear magnetic resonance spectroscopy. Effects of hydrogen bonding and protonation on nitrogen chemical shifts in imidazoles. J. Org. Chem. 44 (1979) 3864–3867.

[15]. Brender JR, Taylor DM, and Ramamoorthy A, Orientation of Amide-Nitrogen-15 Chemical Shift Tensors in Peptides: A Quantum Chemical Study. Journal of the American Chemical Society 123 (2001) 914–922. [PubMed: 11456625]

[16]. Marulanda D, Tasayco ML, McDermott A, Cataldi M, Arriaran V, and Polenova T, Magic angle spinning solid-state NMR spectroscopy for structural studies of protein interfaces. resonance assignments of differentially enriched Escherichia coli thioredoxin reassembled by fragment complementation. J. Am. Chem. Soc. 126 (2004) 16608–20. [PubMed: 15600367]

[17]. Yang J, Paramasivam S, Marulanda D, Cataldi M, Tasayco ML, and Polenova T, Magic angle spinning NMR spectroscopy of thioredoxin reassemblies. Magn. Reson. Chem. 45 Suppl 1 (2007) S73–83. [PubMed: 18157811]

[18]. Sun S, Butterworth AH, Paramasivam S, Yan S, Lightcap CM, Williams JC, and Polenova T, Resonance Assignments and Secondary Structure Analysis of Dynein Light Chain 8 by Magic Angle Spinning NMR Spectroscopy. Can. J. Chem. 89 (2011) 909–918. [PubMed: 23243318]

[19]. Neue G, and Dybowski C, Determining temperature in a magic-angle spinning probe using the temperature dependence of the isotropic chemical shift of lead nitrate. Solid State Nucl. Magn. Reson. 7 (1997) 333–6. [PubMed: 9176939]

Author Manuscript Author Manuscript Author Manuscript Author Manuscript

[20]. Morcombe CR, and Zilm KW, Chemical shift referencing in MAS solid state NMR. J. Magn. Reson. 162 (2003) 479–86. [PubMed: 12810033]

[21]. Chan JCC, Recoupling of chemical shift anisotropies in solid-state NMR under high-speed magic-angle spinning and in uniformly 13C-labeled systems. The Journal of chemical physics 118 8378–8389.

[22]. Gullion T, Baker DB, and Conradi MS, New, compensated Carr-Purcell sequences. J. Magn. Reson. 89 (1990) 479–484.

[23]. Baldus M, Cross polarization in the tilted frame: assignment and spectral simplification in heteronuclear spin systems. Mol. Phys. 95 1197–1207.

[24]. Bennett AE, Heteronuclear decoupling in rotating solids. The Journal of chemical physics 103 6951–6958.

[25]. Bak M, Rasmussen JT, and Nielsen NC, SIMPSON: A General Simulation Program for Solid-State NMR Spectroscopy. J. Magn. Reson. 147 (2000) 296–330. [PubMed: 11097821]

[26]. Bak M, and Nielsen NC, REPULSION, A Novel Approach to Efficient Powder Averaging in Solid-State NMR. J. Magn. Reson. 125 (1997) 132–139. [PubMed: 9245368]

[27]. Wylie BJ, Franks WT, and Rienstra CM, Determinations of 15N Chemical Shift Anisotropy Magnitudes in a Uniformly 15N,13C-Labeled Microcrystalline Protein by Three-Dimensional Magic-Angle Spinning Nuclear Magnetic Resonance Spectroscopy. J. Phys. Chem. B 110 (2006) 10926–10936. [PubMed: 16771346]

[28]. Katti SK, Crystal structure of thioredoxin from Escherichia coli at 1.68 Å resolution. J. Mol. Biol. 212 167–184. [PubMed: 2181145]

[29]. Williams JC, Roulhac PL, Roy AG, Vallee RB, Fitzgerald MC, and Hendrickson WA, Structural and thermodynamic characterization of a cytoplasmic dynein light chain-intermediate chain complex. Proc. Natl. Acad. Sci. USA 104 (2007) 10028–33. [PubMed: 17551010]

[30]. Yan S, Hou G, Schwieters CD, Ahmed S, Williams JC, and Polenova T, Three-dimensional structure of CAP-gly domain of mammalian dynactin determined by magic angle spinning NMR spectroscopy: conformational plasticity and interactions with end-binding protein EB1. J Mol Biol 425 (2013) 4249–66. [PubMed: 23648839]

[31]. Yang J, Tasayco ML, and Polenova T, Dynamics of reassembled thioredoxin studied by magic angle spinning NMR: snapshots from different time scales. J. Am. Chem. Soc. 131 (2009) 13690–702. [PubMed: 19736935]

[32]. Poon A, Birn J, and Ramamoorthy A, How Does an Amide-N Chemical Shift Tensor Vary in Peptides? J. Phys. Chem. B 108 (2004) 16577–16585. [PubMed: 18449362]

Author Manuscript Author Manuscript Author Manuscript Author Manuscript

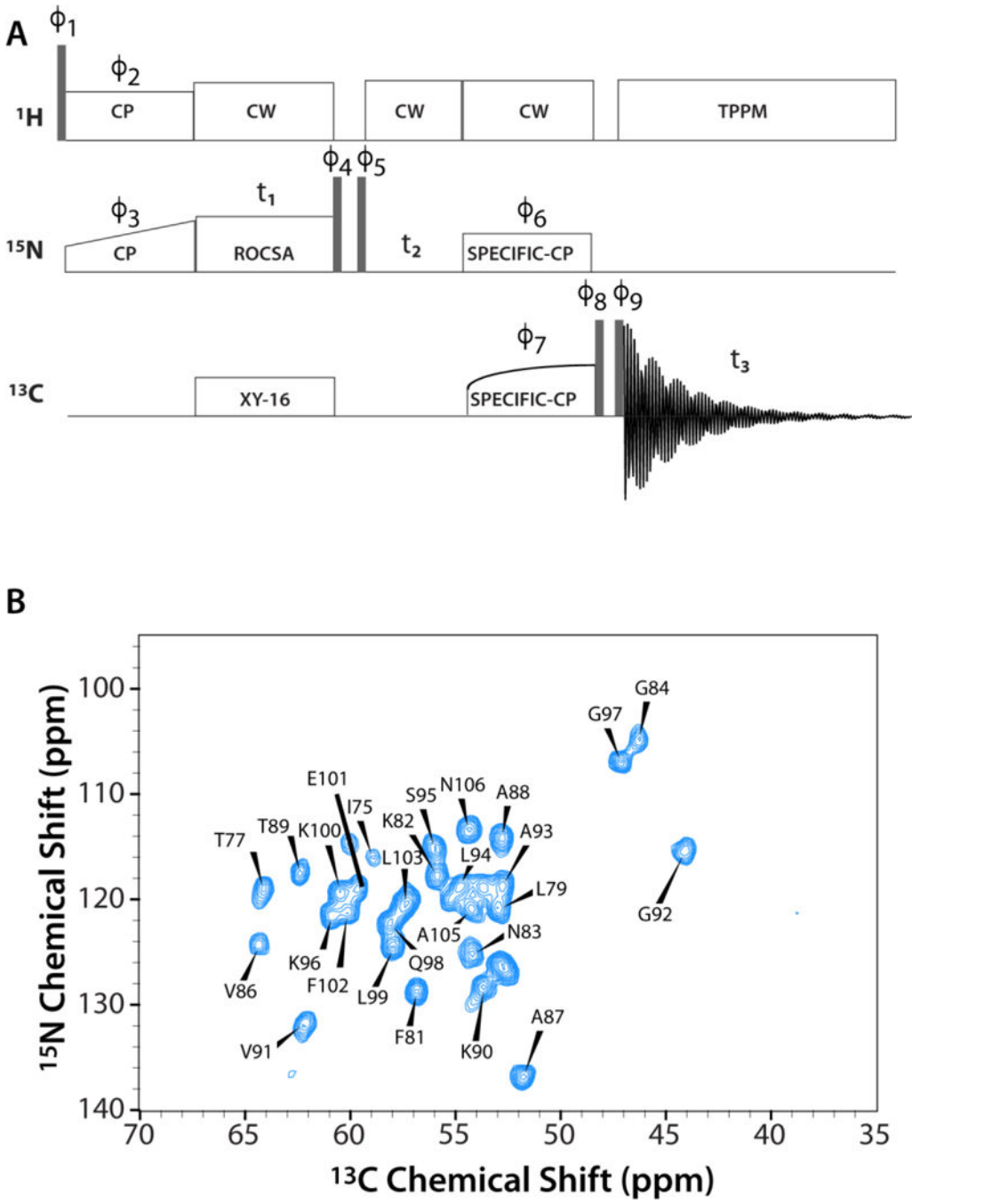

Figure 1.

A) 3D ^{15}N-^{13}CA-ROCSA pulse sequence for site-specific measurement of the backbone amide ^{15}N CSA lineshapes. **B)** The first 2D ^{15}N-^{13}CA plane of the 3D ^{15}N-^{13}CA-ROCSA spectrum of *E. coli* thioredoxin reassembly (U-^{15}N 1–73/^{13}C,^{15}N 74–108).

Author Manuscript Author Manuscript Author Manuscript Author Manuscript

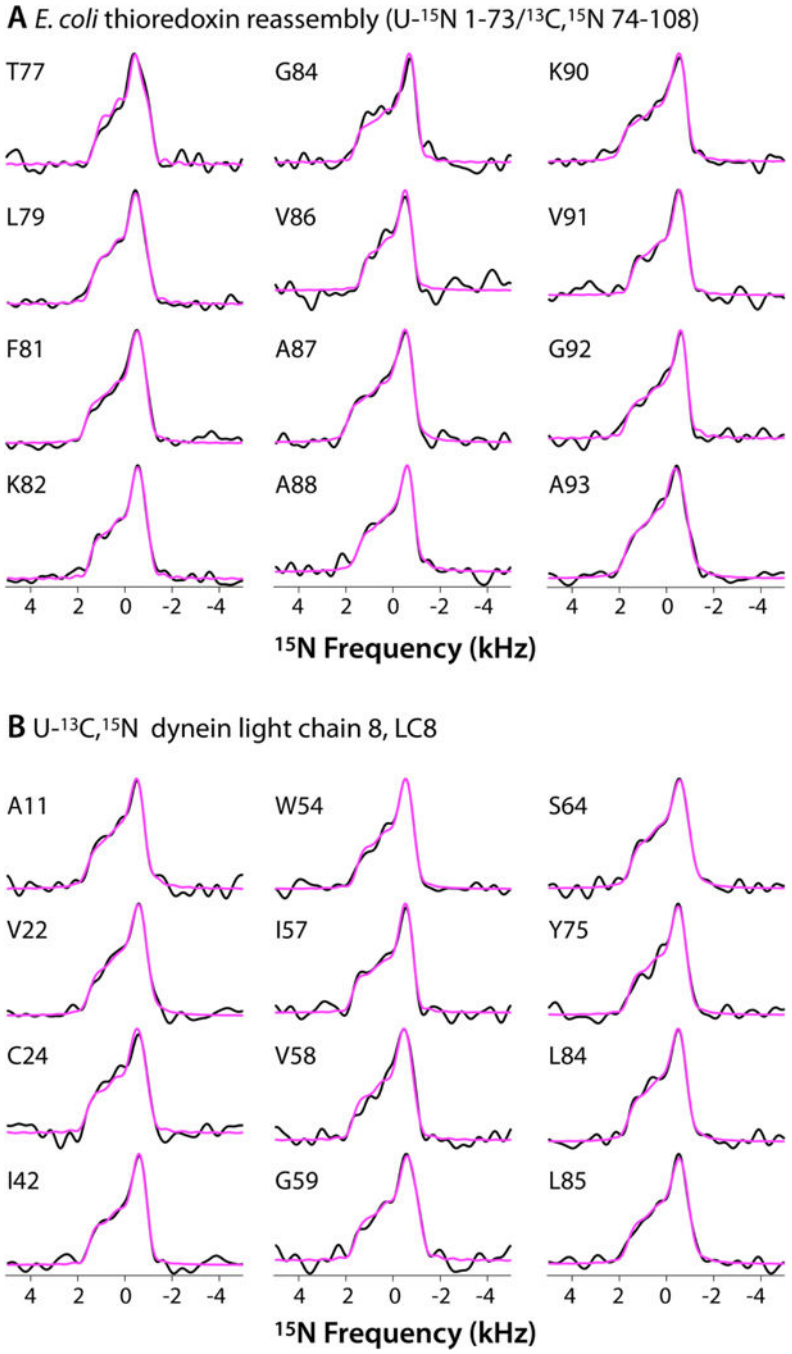

Figure 2.

Representative backbone amide ^{15}N ROCSA lineshapes of **A)** *E. coli* thioredoxin reassembly (U-^{15}N 1–73/^{13}C,^{15}N 74–108) and **B)** dynein light chain 8, LC8.

Author Manuscript Author Manuscript Author Manuscript Author Manuscript

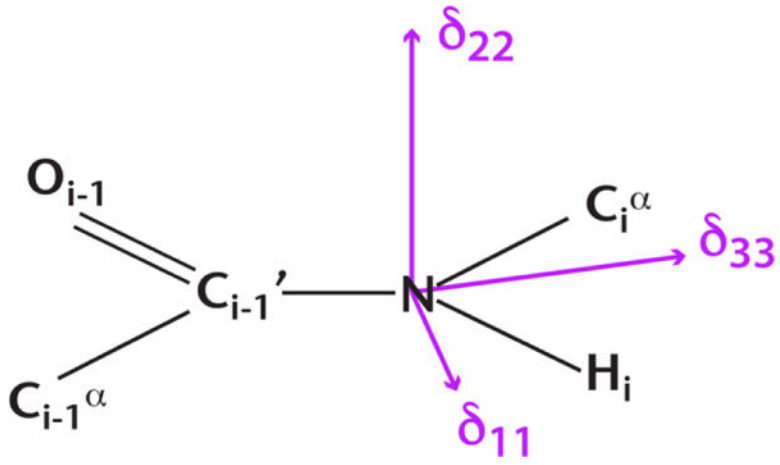

Figure 3.

Illustration of the orientation of the backbone amide ^{15}N CS tensor in the peptide plane (molecular frame). The bond lengths and bond angles are not to scale.

Author Manuscript Author Manuscript Author Manuscript Author Manuscript

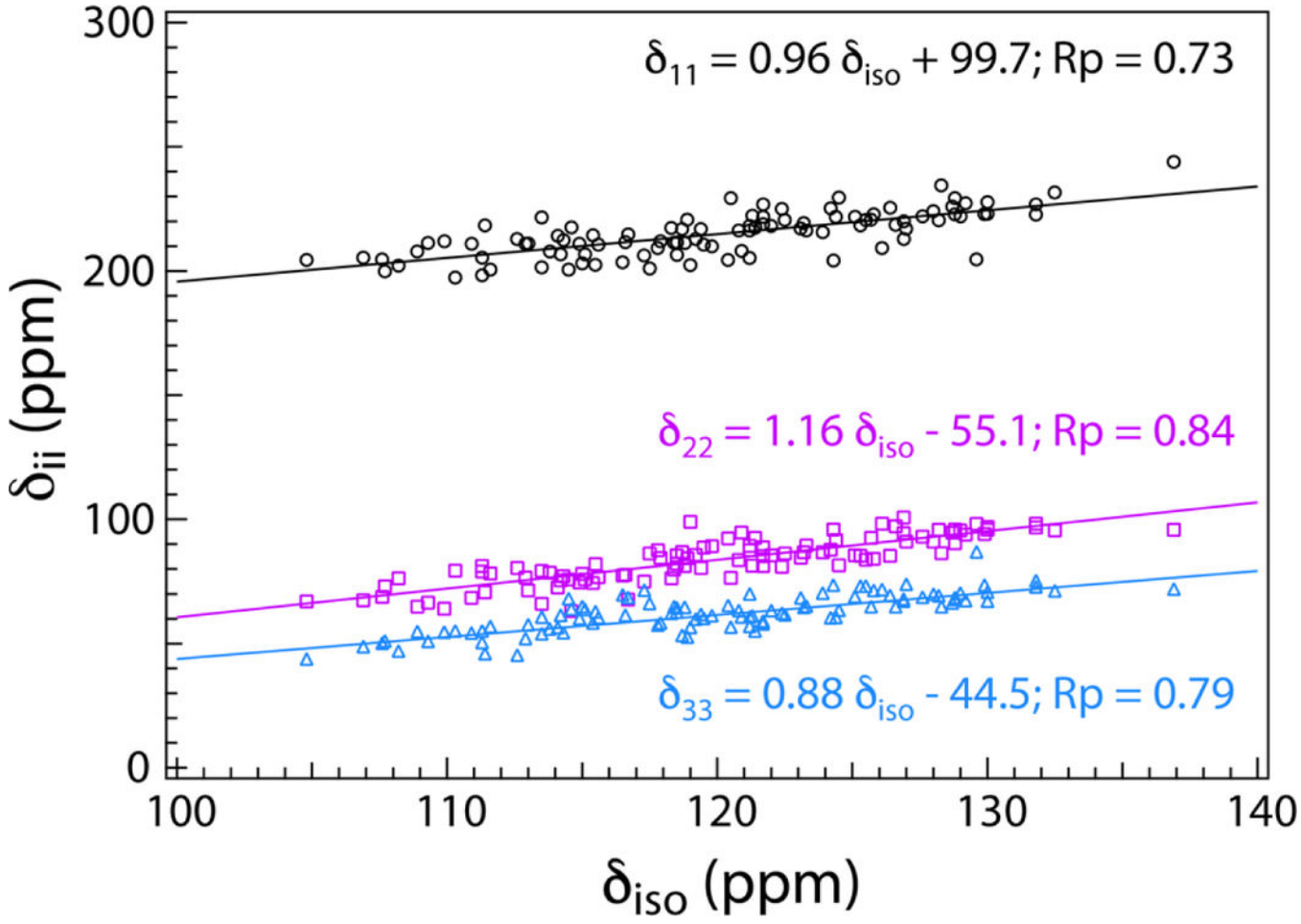

Figure 4.

Correlation of the backbone amide ^{15}N CST principal components with isotropic chemical shift for the four proteins under investigation, *E. coli* thioredoxin reassemblies, LC8, and CAP-Gly. The correlation is determined the Pearson correlation coefficients (R_P) with values greater than 0.70 indicating a strong positive correlation of the three principal components with ^{15}N isotropic chemical shift.

Author Manuscript Author Manuscript Author Manuscript Author Manuscript

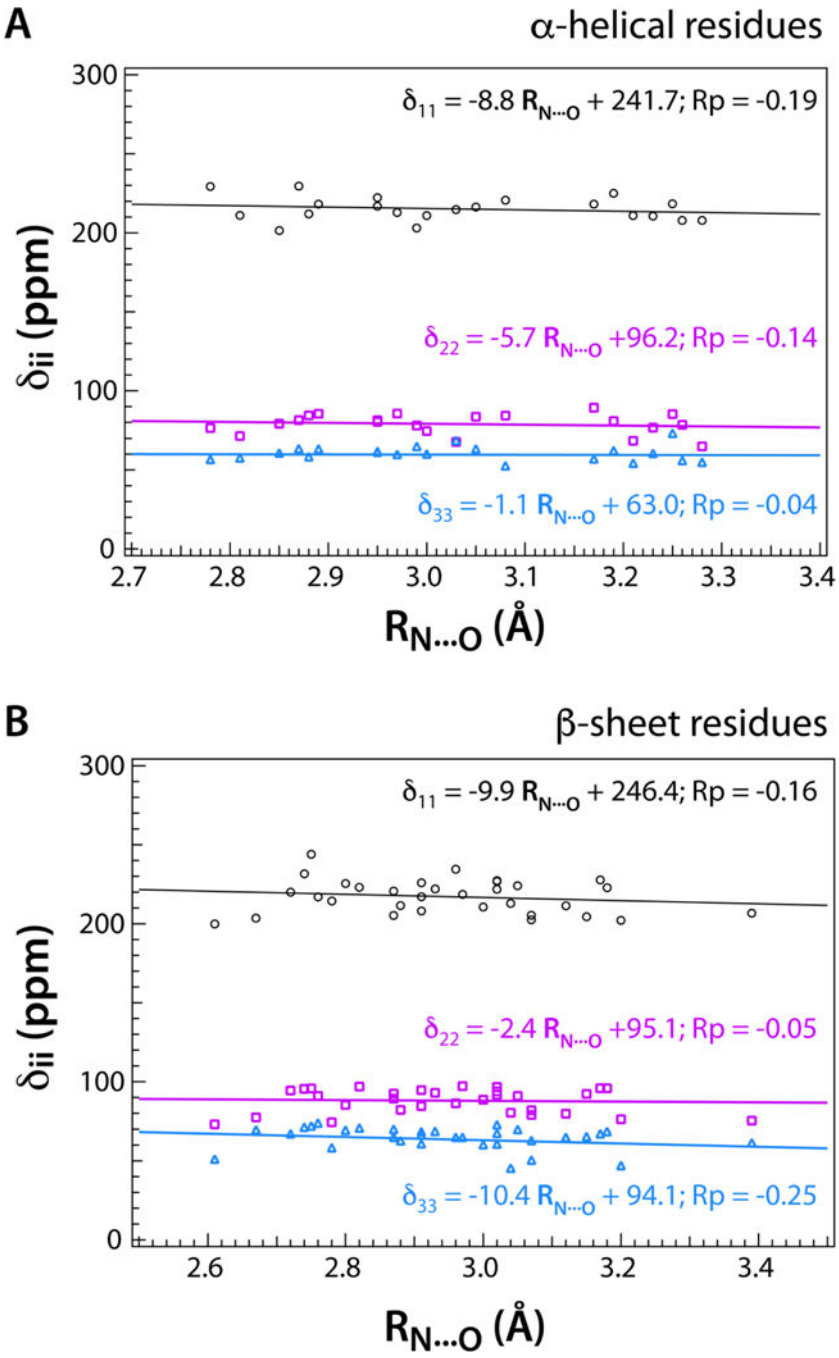

Figure 5.

Correlation of the hydrogen-bonded backbone amide ^{15}N CST principal components with hydrogen bond distance $R_{N...O}$ for **A)** α-helical and **B)** β-sheet structure, for the four proteins under investigation, *E. coli* thioredoxin reassemblies, LC8, and CAP-Gly. The downfield shift of all three ^{15}N CST principal components, notably in δ_{11}, with decreasing $R_{N...O}$ is indicated by the negative Pearson correlation coefficients (R_P) for both α-helical and β-sheet secondary structures.

Author Manuscript

Author Manuscript

Author Manuscript

Author Manuscript

Table 1.

Statistical Averages of the Principal Components of $^{15}N^{H}$ Chemical Shift Tensors for Hydrogen-Bonded and Non-Hydrogen-Bonded Residues of *E. coli* Thioredoxin Reassemblies, LC8, and CAP-Gly.

Type	δ_{iso} (ppm)	δ_{σ} (ppm)	η_{σ}	δ_{11} (ppm)	δ_{22} (ppm)	δ_{33} (ppm)
HB	120.6 ± 6.6	95.8 ± 5.1	0.23 ± 0.08	216.3 ± 8.9	83.8 ± 8.6	61.5 ± 6.6
NHB	118.9 ± 7.1	93.6 ± 7.0	0.24 ± 0.09	212.5 ± 8.8	83.3 ± 10.6	61.0 ± 8.4
Difference	1.7	2.2	–0.01	3.8	0.5	0.5

HB – hydrogen-bonded residues, NHB – non-hydrogen-bonded residues. The values presented here are the statistical average ± standard deviations.